

Observation of an SmC_α^* phase in an antiferroelectric liquid crystal using pyroelectrics and dielectrics

N. M. Shtykov,^{a†} J. K. Vij,^{*a} V. P. Panov,^a R. A. Lewis,^b Michael Hird^b and John W. Goodby^b

^aDepartment of Electronics and Electrical Engineering, Trinity College, University of Dublin, Dublin 2, Ireland. E-mail: jvij@tcd.ie

^bDepartment of Chemistry, University of Hull, Cottingham Road, Hull, UK HU6 7RX

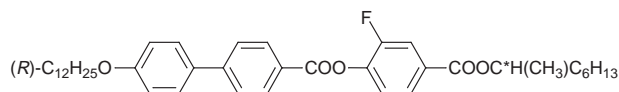
Received 16th March 1999, Accepted 7th May 1999

The measurements of the pyroelectric and dielectric properties as functions of frequency, bias voltage and temperature in the region of the phase transition from the SmA to phases of antiferroelectric liquid crystal (AFLC) are presented. On the basis of the results of pyroelectric and dielectric response, the nature of the SmC_α^* phase in the AFLC material (R)-12OBP1M7 is being established.

The paper reports a study of the SmC_α^* phase using a combination of pyroelectric and dielectric techniques. Antiferroelectric liquid crystals exhibit several subphases between paraelectric smectic A (SmA) and antiferroelectric smectic C_A (SmC_A^*). The subphases in this temperature region were tentatively designated as SmC_α^* , SmC_β^* and SmC_γ^* in order of decreasing temperature.¹ The SmC_β^* phase is usually considered to be the same as the ferroelectric chiral smectic C (SmC^*). Switching characteristics indicate that the SmC_α^* phase is antiferroelectric at temperatures immediately below the phase transition from SmA to SmC_α^* ,² but later electrooptical measurements did not confirm the antiferroelectric behavior of the SmC_α^* phase.³ It was reported that phases SmC_α^* and SmC_γ^* , which have ferrielectric properties, disappear with decreasing optical purity.⁴ The complete investigations of the electric field *versus* temperature (E - T) phase diagrams⁵ for different binary mixtures show that the SmC_α^* phase appears in the temperature range below the SmA and borders with the SmC^* , AF or SmC_γ^* phases. Here AF stands for a high temperature antiferroelectric phase which has a different structure to the SmC_A phase. Neither optical texture nor conoscopic observations are usually effective for the identification of the SmC_α^* phase, but dielectric and electric field-induced apparent tilt angle measurements have proven to be effective in locating the phase transitions to and from the SmC_α^* phase.^{1,6} The appearance and properties of the SmC_α^* phase cannot be explained using the existing theoretical models.^{5,7,8} Although several experimental studies of the SmC_α^* phase have been performed, its structure is still not known. X-Ray diffraction measurements revealed that the SmC_α^* is a tilted smectic phase.⁶ Recently, periodicity incommensurate with the layer spacing has been experimentally detected in the SmC_α^* phase.⁹

In this paper we report the observations of the most interesting dielectric and pyroelectric properties at the phase transition from the SmA to the ferro/antiferroelectric phases and prove that the SmC_α^* phase exists immediately below the SmA phase in the investigated AFLC material (R)-(-)-1-methylheptyl 4-(4'-dodecyloxybiphenyl-4-ylcarbonyloxy)-3-fluorobenzoate, with acronym (R)-12OBP1M7. The final objective of these studies is to find the model for the structure^{9,10} of the phase in antiferroelectric liquid crystals.

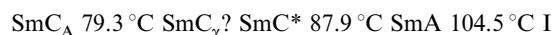
The (R)-12OBP1M7 used in our experiments was synthesized at the University of Hull. Itoh *et al.*¹¹ have investigated similar compounds, but this compound was not



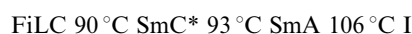
investigated by them. The following phase transition sequence for this material has been found. On using differential scanning calorimetry (DSC), we find that during heating at the rate of 10 K per minute:



and during cooling also at a rate of 10 K per minute:



whereas using conoscopy and spontaneous polarization measurements,^{12,13} the transition temperatures are:



Here AF and FiLC represent phases with antiferroelectric and ferrielectric characteristics, respectively. A large discrepancy first exists between the transition temperatures in heating and cooling rates. This is mainly due to relatively large heating and cooling rates and large relaxation times for some of the ferrielectric phases. One can also observe considerable differences between the phase transition temperatures of SmA to SmC^* obtained by DSC and other methods. We believe that the differences cannot be explained by the fact that DSC uses bulk samples. However conoscopy and polarization measurements are made on thin aligned layers of liquid crystals and the rate of heating and cooling in the latter measurements is 0.1 K per minute.

Dielectric measurements at frequencies from 1 to 40 kHz were made using impedance analyzer HP-4192A. For investigating the macroscopic polarization in different phases of the AFLC material, we used the pyroelectric method given in ref. 14. The temperature measurements were carried out during continuous cooling at the rate of $0.1^\circ\text{C} \ \text{min}^{-1}$. The dependencies of pyroelectric response on bias voltage were measured at the stabilized temperatures at the rate of voltage increase of $0.3 \ \text{V} \ \text{min}^{-1}$.

A cell of 15 μm sample thickness used for dielectric and pyroelectric measurements consisted of two glass plates with ITO (Indium Tin Oxide) layers as electrodes and Mylar thin-film stripes as spacers. The dimensions of the electrodes' working area were $4.5 \times 4.5 \ \text{mm}^2$. Polyimide films (Nissan Chemical Industry, RN-1266) were coated on the ITO electrodes, cured for a duration of 1 h at a temperature of 250°C and then rubbed in one direction by a velvet track to achieve the alignment. The cell was heated and filled with the antiferroelectric compound in the isotropic phase and cooled slowly to the SmA phase.

In order to investigate the phase transition from below the SmA phase, we measured the dependencies of the real part of permittivity, ϵ' , on temperature for different frequencies. Fig. 1

[†]Permanent address: Institute of Crystallography, Russian Academy of Sciences, 117333, Moscow, Leninsky prosp. 59, Russia.

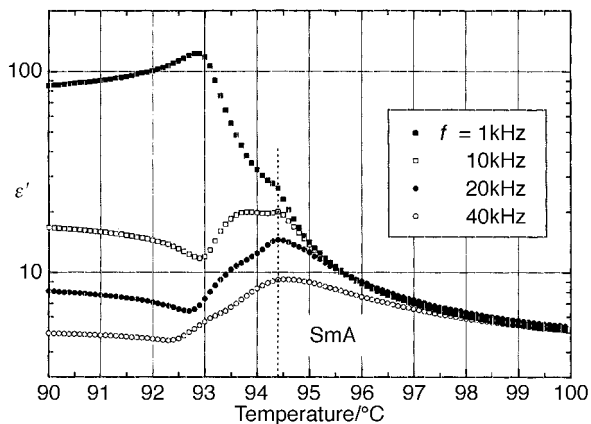


Fig. 1 Temperature dependencies of permittivity ϵ' for different frequencies of measuring voltage.

shows the results of permittivity ϵ' measurements during the cooling scan. The vertical dotted line indicates the temperature of the phase transition from SmA to other phases through the dielectric measurements. For all frequencies ϵ' increases gradually with decreasing temperature in SmA due to the ferroelectric soft mode until the phase transition temperature. The temperature dependence of ϵ' for a measuring frequency of 1 kHz looks like the usual conversion from the soft mode in the SmA phase to the Goldstone mode in the SmC* phase. The soft mode is dominated by the Goldstone mode in SmC* phase. When the frequency of the measurements is increased, ϵ' in the SmC* phase decreases due to the dispersion arising from the Goldstone mode. But in the region of 1–1.5 °C immediately below the phase transition from SmA the value of ϵ' remains fairly large and cannot be explained by the presence of only the soft mode as shown in Fig. 2. Fig. 2 also shows the temperature dependence of ϵ' for a measuring frequency of 40 kHz, the soft mode contribution (ϵ'_{sm}) in the total permittivity ϵ' and their difference $\delta\epsilon' = \epsilon' - \epsilon'_{sm}$ below the phase transition temperature. The soft mode contribution in SmA is obtained using fitting of the experimental data on ϵ' by eqn. (1),

$$\epsilon'(T) = \epsilon + \epsilon'_{sm}(T) = \epsilon + \frac{A}{T - T_c + B} \quad (1)$$

where ϵ is the conventional permittivity, excluding the contribution from collective modes, $T_c = 94.5$ °C is the phase transition temperature, A and B are fitting parameters. These are found to be $A = 23.5$ [K], $B = 3.0$ [K]. The detailed expressions of A and B in terms of the parameters of Landau's phenomenological theory for phase transitions can be found elsewhere.¹⁵ For temperatures below the phase transition, the soft mode

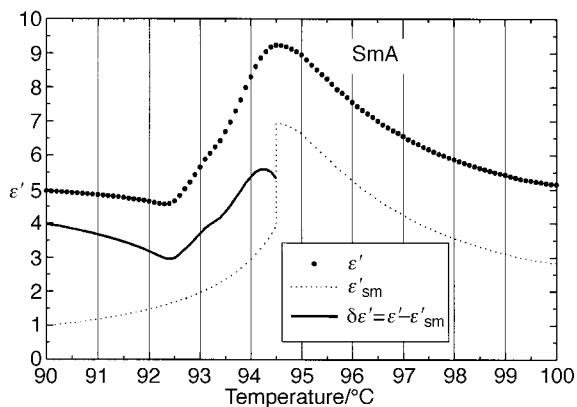


Fig. 2 Dependencies on temperature of total permittivity ϵ' for frequency 40 kHz, soft mode contributions ϵ'_{sm} in SmA and below the phase transition temperature and their differences $\delta\epsilon' = \epsilon' - \epsilon'_{sm}$ in the SmC $_{\alpha}^*$ and SmC* phases.

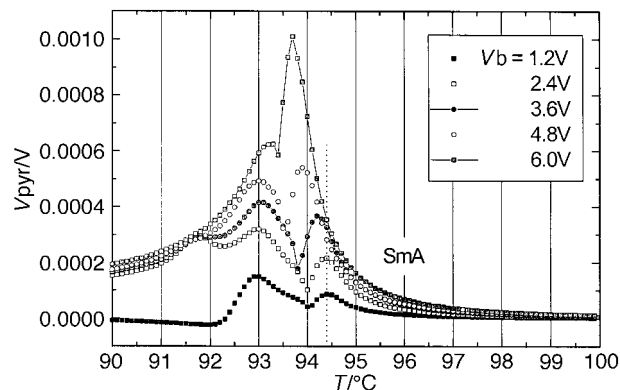


Fig. 3 Pyroelectric response as a function of temperature for various bias voltages.

contribution was calculated (using values of A and B found in the SmA phase) using an analogous expression [eqn. (2)] for the SmC* phase.¹³

$$\epsilon'_{sm}(T) = \frac{0.25A}{T_c - T + 0.5B} \quad (2)$$

As seen from Fig. 2, the behavior of ϵ' immediately below the phase transition from SmA is not typical for the Goldstone mode. The Goldstone mode in the SmC* phase increases with increasing spontaneous polarization and helical pitch. However Fig. 2 shows that the strength of this mode decreases with temperature. Therefore we can assume that the SmC $_{\alpha}^*$ phase does exist immediately below the phase transition from SmA. We confirm the deduction of Hiraoka *et al.*³ that another ferroelectric mode, in addition to the soft mode associated with the tilt fluctuations, exists in the SmC $_{\alpha}^*$ phase. The pyroelectric response also shows unusual behavior at the phase transition from the SmA to the SmC* phase. Temperature dependencies of the pyroelectric signal for some bias voltages are given in Fig. 3. We see that the curves have two peaks (three peaks for some values of the bias voltage). The peaks move closer with an increase of bias voltage. This fact obviously implies that the temperature region of the SmC $_{\alpha}^*$ phase decreases with bias voltage due to the field induced phase transitions from the SmC $_{\alpha}^*$ to the SmC* phase, at lower temperatures, and from the SmC $_{\alpha}^*$ to the SmA phase at higher temperatures. The first peak for the least bias voltage coincides with the phase transition temperature from the SmA to the SmC $_{\alpha}^*$ phase (94.5 °C) determined for zero bias voltage by the dielectric measurements. The second peak appears to indicate the phase transition from the SmC $_{\alpha}^*$ to the SmC* phase (93 °C). The stepwise dependence of the pyroelectric response on the bias voltage (Fig. 4, curves c, d) also confirms our assumption that the SmC $_{\alpha}^*$ phase really exists in (R)-12OBP1M7 in the temperature range from 94.5 to 93 °C.

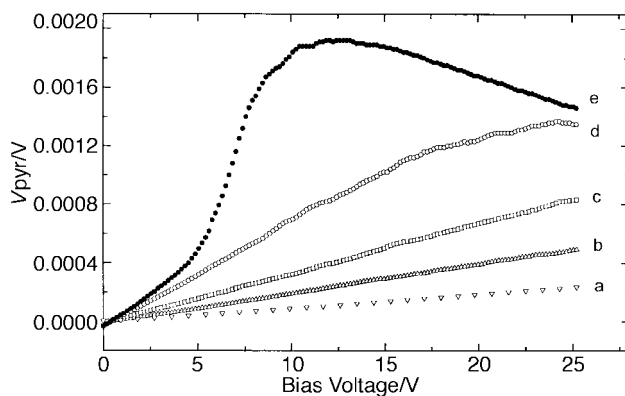


Fig. 4 Dependence of the pyroelectric signal on the bias voltage for various temperatures in SmA [(a) 95 °C, (b) 94.5 °C] and SmC $_{\alpha}^*$ [(c) 94 °C, (d) 93.5 °C, (e) 93 °C] phases.

Fig. 4 shows the voltage dependencies of the pyroelectric response in the SmA (curves a, b) and the SmC_α^* (curves c–e) phases. As seen from Fig. 4, the shapes of the curves depend not only on the phase but also on the temperature within the phase. The three curves 94, 93.5 and 93 °C correspond to the SmC_α^* phase but these exhibit different shapes. At 94 °C the curve shows a typical dependence of the pyroelectric response on voltage for the paraelectric SmA phase (curves a, b), where the pyroelectric response is found to be linearly related to voltage. Curve (d) demonstrates a stepwise increase of the pyroelectric response which at higher voltages reaches the saturation value, as does the apparent tilt angle *versus* electric field in ref. 6. In the case of curve (e) at low voltages the pyroelectric response linearly increases with voltage and then a field-induced phase transition from SmC_α^* to SmC^* occurs as indicated by a deviation from the linear relationship with bias voltage. In the SmC_α^* phase the level of the induced tilt angle and therefore the value of the pyroelectric response is strongly dependent on temperature.⁶ We find that the pyroelectric response in SmC_α^* is non-linear. This implies that the spontaneous polarization rises in small steps with an increase in voltage. This means that SmC_α^* is a tilted phase and the neighbouring layer structure constantly fluctuates between those governed by the ferroelectric and the antiferroelectric states. The behaviour is different from a ferroelectric phase.

This work was supported by the European ORCHIS network and partly by RFBR grant 98–02–17071.

Notes and references

- 1 A. Fukuda, Y. Takanishi, T. Isozaki, K. Ishikawa and H. Takezoe, *J. Mater. Chem.*, 1994, **4**, 997.
- 2 T. Isozaki, Y. Suzuki, I. Kawamura, K. Mori, N. Yamamoto, Y. Yamada, H. Orihara and Y. Ishibashi, *Jpn. J. Appl. Phys.*, 1991, **30**, L1573.
- 3 K. Hiraoka, Y. Uematsu, H. Takezoe and A. Fukuda, *Jpn. J. Appl. Phys.*, 1996, **35**, 6157.
- 4 M. Fukui, H. Orihara, Y. Yamada, N. Yamamoto and Y. Ishibashi, *Jpn. J. Appl. Phys.*, 1989, **28**, L849.
- 5 T. Isozaki, T. Fujikawa, H. Takezoe, A. Fukuda, T. Hagiwara, Y. Suzuki and I. Kawamura, *Jpn. J. Appl. Phys.*, 1992, **31**, L1435.
- 6 K. Hiraoka, Y. Takanishi, K. Skarp, H. Takezoe and A. Fukuda, *Jpn. J. Appl. Phys.*, 1991, **30**, L1819.
- 7 M. Yamashita and S. Miyazima, *Ferroelectrics*, 1993, **148**, 1.
- 8 J. Prost and R. Bruinsma, *Ferroelectrics*, 1993, **148**, 9.
- 9 P. Mach, R. Pindak, A.-M. Levelut, P. Barois, H. T. Nguyen, C. C. Huang and L. Furenid, *Phys. Rev. Lett.*, 1998, **81**, 1015.
- 10 M. Čepič and B. Žekš, *Mol. Cryst. Liq. Cryst.*, 1995, **263**, 61.
- 11 K. Itoh, M. Kabe, K. Miyachi, Y. Takanishi, K. Ishikawa, H. Takezoe and A. Fukuda, *J. Mater. Chem.*, 1997, **7**, 407.
- 12 Yu. P. Panarin, O. Kalinovskaya, J. K. Vij and J. W. Goodby, *Phys. Rev. E*, 1997, **55**, 4353.
- 13 J. W. O'Sullivan, Yu. P. Panarin, J. K. Vij, A. J. Seed, M. Hird and J. W. Goodby, *J. Phys. Condens. Mater.*, 1996, **8**, L551.
- 14 J. W. O'Sullivan, Yu. P. Panarin and J. K. Vij, *J. Appl. Phys.*, 1995, **77**, 1201.
- 15 P. Martinot-Lagarde and G. Durand, *J. Phys. (Paris)*, 1981, **42**, 269.

Communication 9/02055A